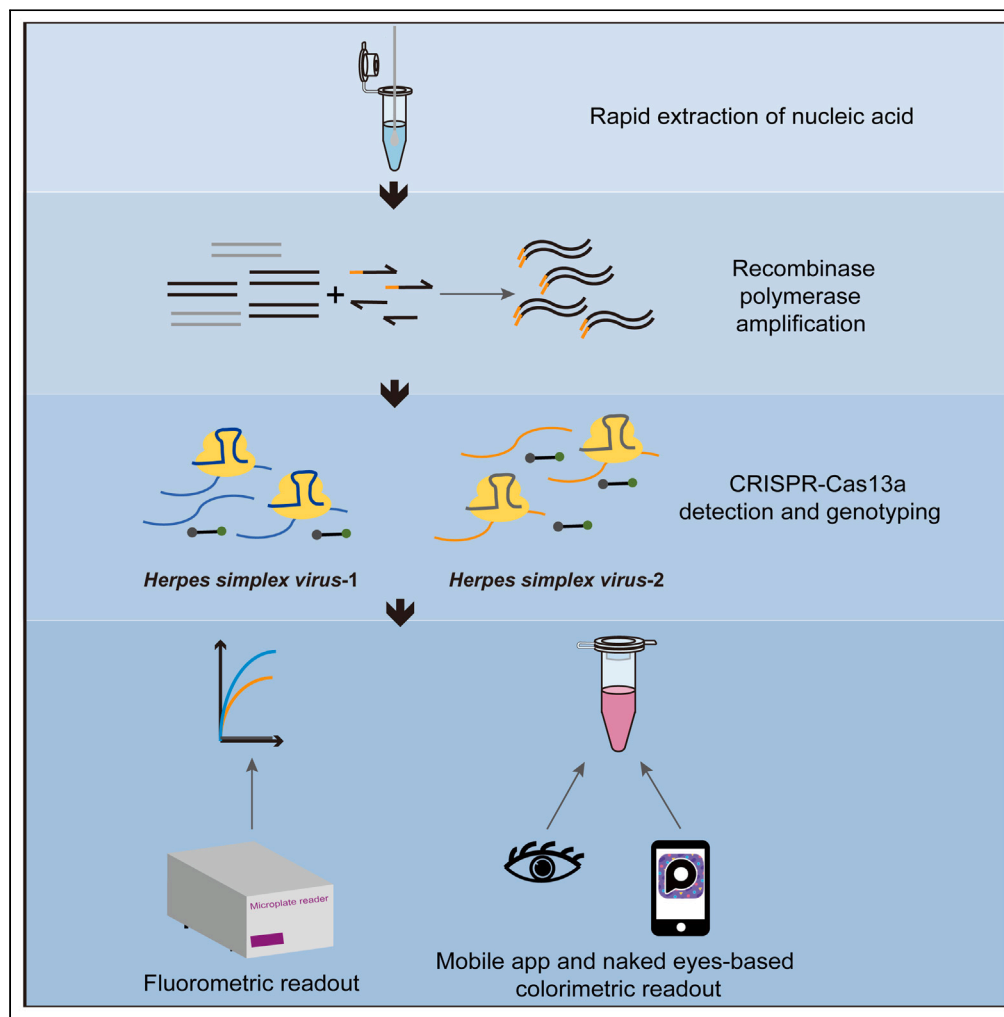


Article

A rapid isothermal CRISPR-Cas13a diagnostic test for genital *herpes simplex virus* infection

Xiaona Yin, Hao Luo, Han Zhou, ..., Zhanqin Feng, Wentao Chen, Heping Zheng

wentao_c@hotmail.com (W.C.)
zhengheping@smu.edu.cn (H.Z.)

Highlights

An isothermal CRISPR-Cas13a assay for genital HSV detection and genotyping

High sensitivity, specificity, and comparative performance with qPCR in 194 samples

Diversified readouts—fluorometric or naked-eye colorimetric detection

Article

A rapid isothermal CRISPR-Cas13a diagnostic test for genital *herpes simplex virus* infection

Xiaona Yin,^{1,2} Hao Luo,^{1,2} Han Zhou,^{1,2} Ziyang Zhang,^{1,2} Yinyuan Lan,^{1,2} Zhanqin Feng,^{1,2} Wentao Chen,^{1,2,3,*} and Heping Zheng^{1,2,4,*}

SUMMARY

Prompt diagnosis is essential for managing *herpes simplex virus* types 1 and 2 (HSV-1/2). Existing diagnostic methods are not widely available that required expensive or additional equipment for conducting examinations and result readouts, which can limit their utility in resource-constrained settings. We successfully developed a CRISPR-Cas13a-based assay for the detection and genotyping of HSV. Our assay demonstrated a high sensitivity of 96.15% and 95.15% for HSV-1 and HSV-2, respectively, with a specificity of 100% compared to a commercial qPCR assay when tested on 194 clinical samples. Remarkably, the assay enables a limit of detection of 1 copy/ μ L of viral DNA, facilitated by an enhanced input of RPA product and is designed for both mobile app integration and colorimetric interpretation, allowing for semiquantitative readings. These findings highlight the excellent performance of our CRISPR-based diagnostic in detecting HSV and its potential for point-of-care testing in resource-constrained settings.

INTRODUCTION

Herpes simplex virus (HSV), which belongs to the *Herpesviridae* family, encompasses HSV type 1 (HSV-1) and HSV type 2 (HSV-2).^{1,2} HSV-2 infections commonly result in genital herpes, while HSV-1 is increasingly identified as a causative agent, leading to recurrent infections and lifelong latency.^{3–5} According to the World Health Organization, an estimated 3.7 billion individuals younger than 50 were living with HSV-1 infection in 2016, accounting for approximately 67% of the global population.⁶ Approximately 25% of HSV-1 infections in the age group of 15–49 are estimated to be associated with genital infections.⁷ Additionally, it was found that 491.5 million individuals aged 15 to 49 years were infected with HSV-2, representing around 13.2% of the world's population.⁶ Furthermore, in 2019, the economic burden of HSV infections was estimated to be 212 billion in 90 low- and middle-income countries (LMICs).⁸ To ensure appropriate treatment, prognosis, and patient guidance, genotyping should be conducted at the initial stage of genital herpes since HSV-1 and HSV-2 cannot be feasibly differentiated in the clinic.^{4,9}

The traditional cell culture-based assay is widely regarded as the gold standard for virologic diagnosis of HSV infection.¹⁰ However, its application in clinical laboratories is hindered by several factors, as the assay is time-consuming, involves intensive labor, and exhibits limited sensitivity, which limit its practicality.^{11,12} Nucleic acid amplification tests (NAATs), such as qPCR¹³ and droplet digital PCR,¹⁴ are widely acknowledged as the most sensitive diagnostic tests for detecting HSV in various clinical scenarios.^{15–17} They offer high sensitivity for detecting HSV in genital ulcers and mucocutaneous lesions, as well as HSV infections that affect the central nervous system and systemic infections.^{7,18} Nevertheless, importantly, NAATs necessitate the use of a thermal cycler to facilitate cycling through different temperatures, and the result can be complex and difficult to interpret.¹⁹ These factors can pose challenges for implementation, particularly in resource-constrained areas in which access to sophisticated laboratory equipment and technical expertise may be limited.²⁰ To address the reliance on thermal cyclers, a technique called loop-mediated isothermal amplification (LAMP) has been developed for HSV detection, eliminating the need for temperature cycling.²¹ However, it should be noted that LAMP assays can be prone to generating false positive amplification due to the complex design involving four to six primers.²² Previous research has advanced HSV point-of-care testing (POCT) by enabling visual results; however, the sensitivity of these assays varies across different genotypes. Notably, the IsoAMP assay's sensitivity for HSV-2 detection is six times lower than that for HSV-1.²³ Conversely, the LAMP method displays a stark contrast in sensitivities, with its detection efficacy for HSV-1 being a hundred times less than for HSV-2.²¹

CRISPR-based diagnostic assays have emerged as a promising avenue for diagnosis of infectious diseases.^{24,25} Notably, techniques such as specific high-sensitivity enzymatic reporter unlocking (SHERLOCK) and PCR-LwCas13a achieve remarkable performance in pathogen detection by combining recombinase polymerase amplification (RPA) or PCR with Cas13a technology.^{26,27} These advancements have shown excellent diagnostic capabilities for various pathogens, including *Zika virus*,²⁷ *dengue virus*,²⁷ *human immunodeficiency virus*,²⁸ *Treponema*

¹Dermatology Hospital, Southern Medical University, Guangzhou 510091, China

²Guangzhou Key Laboratory for Sexually Transmitted Diseases Control, Guangzhou 510091, China

³Guangdong Provincial Key Laboratory of Tropical Disease Research, School of Public Health, Southern Medical University, Guangzhou 510515, China

⁴Lead contact

*Correspondence: wentao_c@hotmail.com (W.C.), zhengheping@smu.edu.cn (H.Z.)

<https://doi.org/10.1016/j.isci.2023.108581>



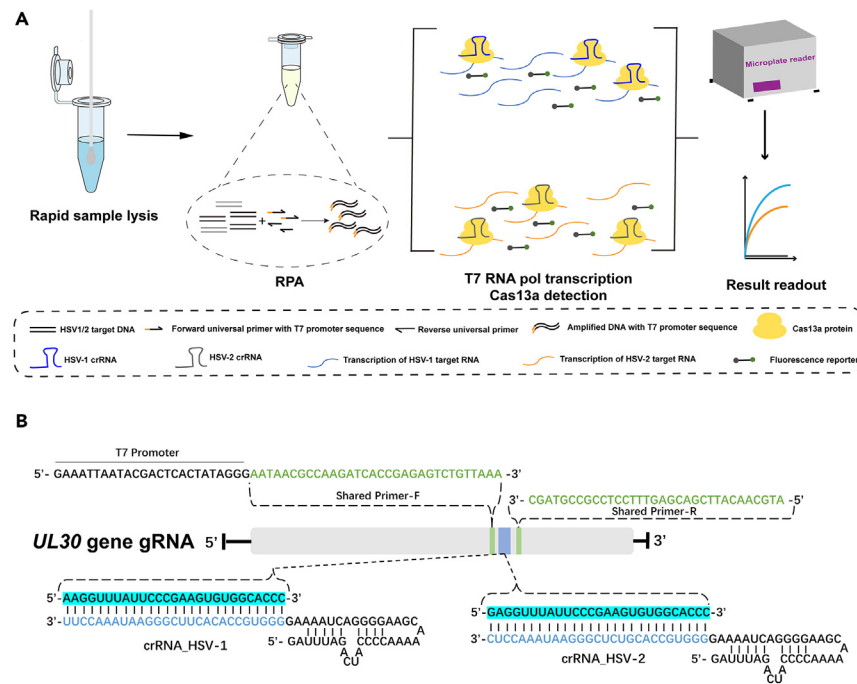


Figure 1. Herpes simplex virus detection and genotyping with the SHERLOCK assay

(A) SHERLOCK dual-target diagnostic herpes simplex virus workflow. (1) Clinical samples were incubated at 100°C for 10 min for DNA extraction. (2) The target gene of HSV-1 or HSV-2 is preamplified with a set of universal primers by RPA in a single tube with extracted DNA as the input. (3) RPA products were further transferred to the separate tubes containing target-specific crRNA for Cas13a detection. (4) The fluorescence readout results were recorded using a microplate reader.

(B) Design of the optimal RPA universal primers and crRNAs for the specific HSV targets. The forward primers contain a T7 promoter for transcription, and the crRNAs consist of a 28 nt spacer complementary to the target and core sequence for binding to the Cas13a protein.

pallidum,²⁶ *Neisseria gonorrhoeae*,²⁹ and severe acute respiratory syndrome coronavirus 2.³⁰ Additionally, researchers have significantly advanced the SHERLOCK technique by integrating it with smartphones,³¹ microfluidic chips,³² and electrochemical sensors.³³ These adaptations enable handheld detection, showcasing the potential for POCT and utilization in resource-constrained settings. Wu et al. have introduced a digital CRISPR-Cas12b-based method for the quantitative detection of HSV,³⁴ whereas Dou and colleagues have elucidated a CRISPR-Cas12a-based approach for the detection of HSV-1 in serum.³⁵ However, it is noteworthy that existing CRISPR-based diagnostic techniques, which rely on Cas12, lack a comprehensive evaluation involving a substantial clinical sample cohort. Furthermore, these methods currently do not possess the capability to differentiate between various HSV subtypes.

In our study, we developed an isothermal assay for the detection and genotyping of HSV by integrating RPA with a dual-target CRISPR-Cas13a system. To reduce reliance on specialized readout equipment and mitigate the subjectivity of visual result interpretation, we introduced a user-friendly smartphone app called "Palette Cam" for result analysis. The assay was convenient to use and its performance was excellent, offering a potential tool for accurately detecting and genotyping HSV in underdeveloped regions of the world.

RESULTS

HSV-SHERLOCK for detection and genotyping of herpes simplex viruses

SHERLOCK, with its combination of RPA and Cas13a technology, is an outstanding diagnostic method.²⁷ To construct an SHERLOCK assay for HSV detection and genotyping, we initially designed CRISPR RNAs (crRNAs) targeting eight different sites within the *UL30* gene of HSV-1 and HSV-2 (Figure S1A). The efficiency of target cleavage by crRNAs was evaluated using double-stranded DNA (dsDNA) of the *UL30* gene as templates. The results indicated that crRNA8 exhibited the highest fluorescence efficiency and specificity for both types of HSV (Figure S1B). Subsequently, the length of crRNA8 was optimized, with 28 nucleotides determined to be the most effective in terms of fluorescence efficiency (Figure S1C). Additionally, a screening process involving six universal forward primers containing the T7 promoter (F1 to F6) and six universal reverse primers (R1 to R6) was conducted for the RPA reaction using the LwCas13a collateral reaction with the optimal crRNA. Among the 36 possible primer combinations, the F3 and R3 primer pair was selected based on the amplification efficiency of both HSV types (Figure S1D). Thus, through successful screening and selection, we established the optimal primers and crRNA for our isothermal amplification and Cas13a detection system (Figure 1B).

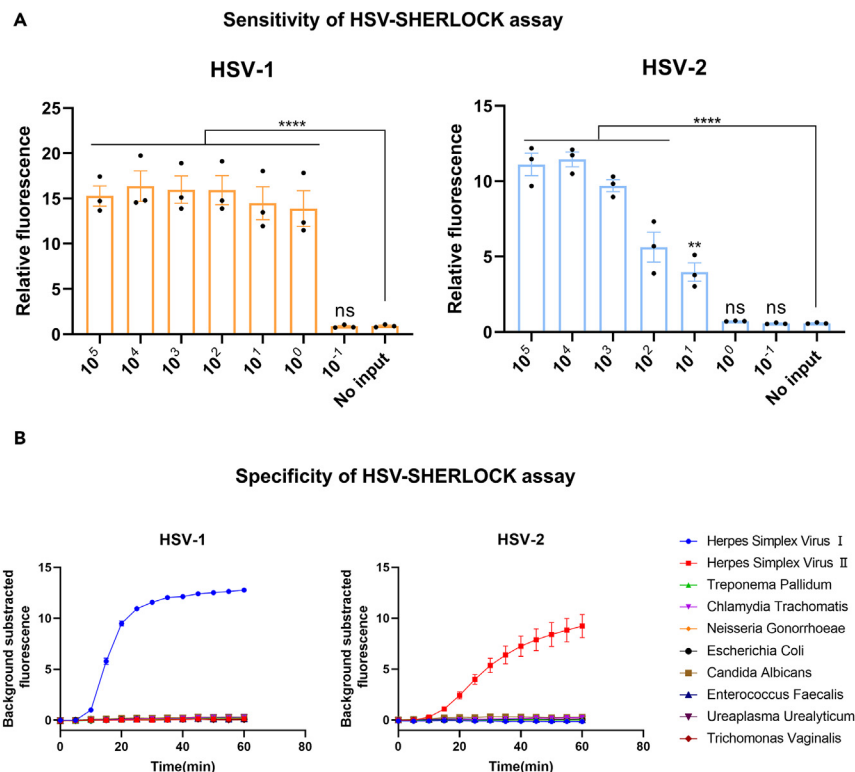


Figure 2. Evaluation of the sensitivity and specificity of the HSV-SHERLOCK assay

(A) Sensitivity of the HSV-SHERLOCK assay was determined by using a 10-fold serial dilution from 10⁵ to 10⁻¹ copies/μL of the double-stranded DNA template (error bars represent the mean ± SEM, where n = 3 replicates). Data were analyzed by one-way ANOVA to compare the mean of each column with the mean of the no input column. * = p < 0.05; ** = p < 0.01; *** = p < 0.001; **** = p < 0.0001; ns = not significant.

(B) Specificity assessment of the HSV-SHERLOCK assay for HSV detection with a panel of ten prevalent urogenital pathogens (error bars represent the mean ± SEM, where n = 3 replicates).

The nucleic acid of clinical samples was extracted with a boiling pyrolysis process, accomplished by heating them to a temperature of 100°C for a period of 10 min. Subsequently, the target genes of HSV-1 and HSV-2 were amplified by utilizing universal primers containing a T7 promoter. The amplification process was carried out at 37°C for 1 h. Following amplification, the resulting RPA products were transferred into separate tubes containing crRNA specific to HSV-1 and HSV-2. The T7 RNA polymerase recognized the T7 promoter on the amplified DNA, and transcribed the amplified DNA into RNA. Subsequently, Cas13a cleaved the RNA guided by crRNA and detected the transcribed RNA targets by releasing RNA reporter signal via Cas13a "collateral" cleavage, which involves the activated Cas13a protein indiscriminately cleaving surrounding non-target RNA. After incubation at 37°C for 1 h, the final results were obtained by fluorescence detection using a fluorescent reader (Figure 1A).

Robust sensitivity and specificity of the HSV-SHERLOCK assay

To assess the sensitivity of HSV-SHERLOCK, we produced dsDNA of the *UL30* gene for HSV-1 and HSV-2 as the reference standard. To simulate the background of a clinical sample, we added 1 ng of HeLa cell DNA to a series of dilutions of dsDNA samples ranging from 10⁵ to 10⁻¹ copies/μL. For RPA amplification, a volume of 1 μL from each standard sample with different copy numbers was added, followed by Cas13a collateral detection. The limit of detection achieved with our assay was 1 copy per reaction of HSV-1 and 10 copies per reaction of HSV-2 (Figure 2A).

To evaluate the specificity of this new assay, we tested it using a panel of common urogenital microorganisms, including *herpes simplex virus I*, *herpes simplex virus II*, *Treponema pallidum*, *Chlamydia trachomatis*, *Neisseria gonorrhoeae*, *Escherichia coli*, *Candida albicans*, *Enterococcus faecalis*, *Ureaplasma urealyticum*, and *Trichomonas vaginalis*. No cross-reactivity with other urogenital pathogens was observed during testing, indicating the excellent specificity of HSV-SHERLOCK (Figure 2B).

Excellent performance of HSV-SHERLOCK in detecting clinical samples

To evaluate the performance of the HSV-SHERLOCK assay, we conducted testing using a total of 194 clinical samples with a known HSV status. The results obtained from the HSV-SHERLOCK assay were compared with those of a commercially available qPCR kit currently used to

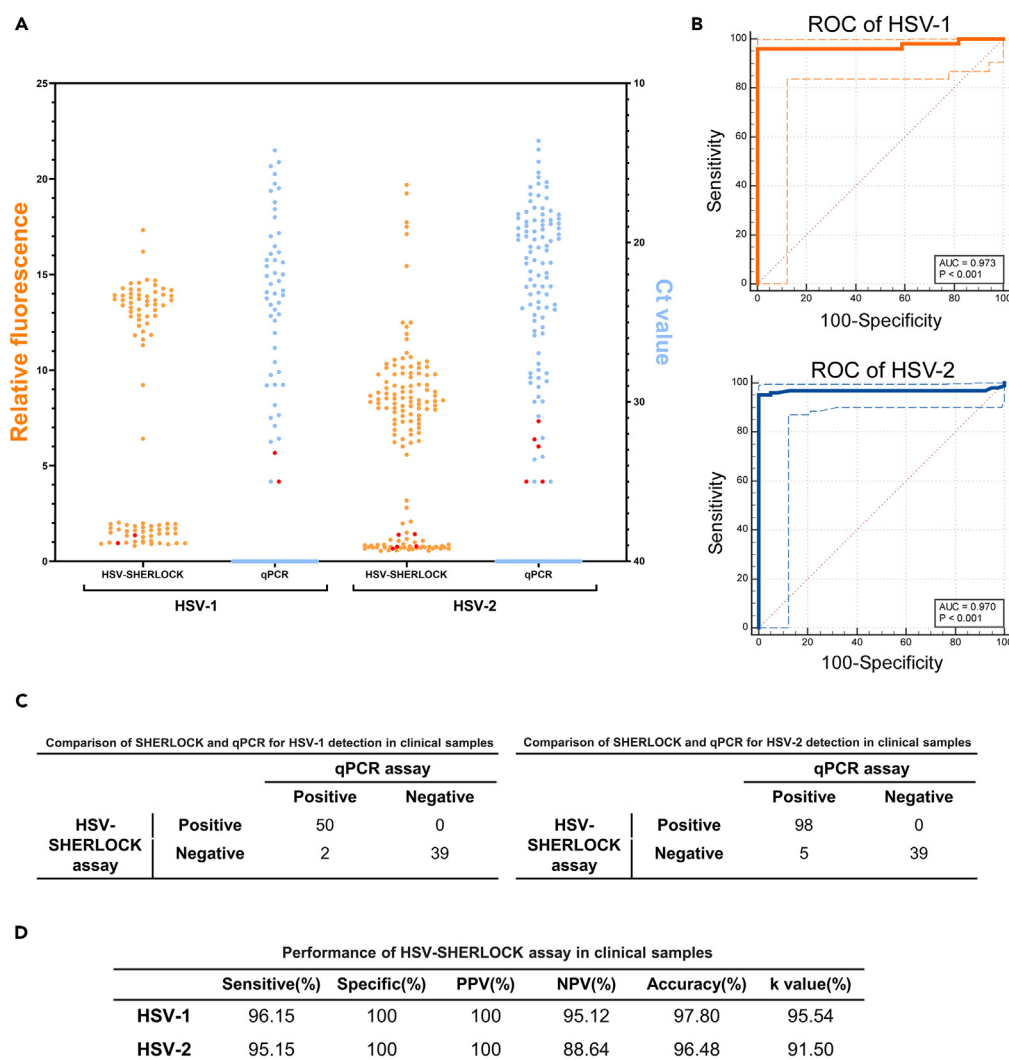


Figure 3. The performance of the HSV-SHERLOCK assay in detecting and genotyping clinical samples

(A) The fluorescence readout results for HSV1/2 with FAM reporter. The left columns represent the results of the HSV-SHERLOCK assay with relative fluorescence value and the right columns display the clinical qPCR detection results with Ct values. The red dots represent clinically discrepant samples between the HSV-SHERLOCK assay and the qPCR kit detection.

(B) ROC curve for HSV-SHERLOCK assay detection in 194 clinical samples. The solid line represents the ROC curve, the dashed line represents the confidence interval of the ROC curve, and the red dashed line represents the diagonal line.

(C) The results obtained for HSV detection with the HSV-SHERLOCK assay and the commercial qPCR kit.

(D) Table containing the results of specificity, sensitivity, PPV, NPV, accuracy, and k value was obtained from comparison of HSV-SHERLOCK and the commercial qPCR kit in clinical samples.

diagnose HSV in the clinical setting. The HSV-SHERLOCK assay exhibited a sensitivity of 96.15% (95% CI = 86.8–99.5) and a specificity of 100% (95% CI = 91–100) for HSV-1, as well as a sensitivity of 95.15% (95% CI = 92.7–99.1) and a specificity of 100% (95% CI = 91–100) for HSV-2, when using a fluorescence readout (Figure 3A). Receiver operating characteristic curves were generated, and the area under the curve (AUC) for detecting HSV-1 was 0.973 (95% CI = 0.915 to 0.996), while the AUC for detecting HSV-2 was 0.970 (95% CI = 0.927 to 0.991) (Figure 3B). These results indicate the assay exhibits excellent discriminatory power and accuracy for laboratory diagnosis of HSV-1 and HSV-2 infections. The positive predictive value (PPV), negative predictive value (NPV), accuracy, and kappa value results further support the robust performance of the developed system for detecting HSV-1 and HSV-2 infections (Figures 3C and 3D).

Adapting HSV-SHERLOCK for convenient visualization

To create a visual reaction system, we replaced the fluorescent moiety with an eye-visible ROX on the RNA reporter to facilitate visual detection in HSV-SHERLOCK. Different concentrations of ROX probes (5, 10, 20, 25, and 30 μ M) were tested in the system, and the color

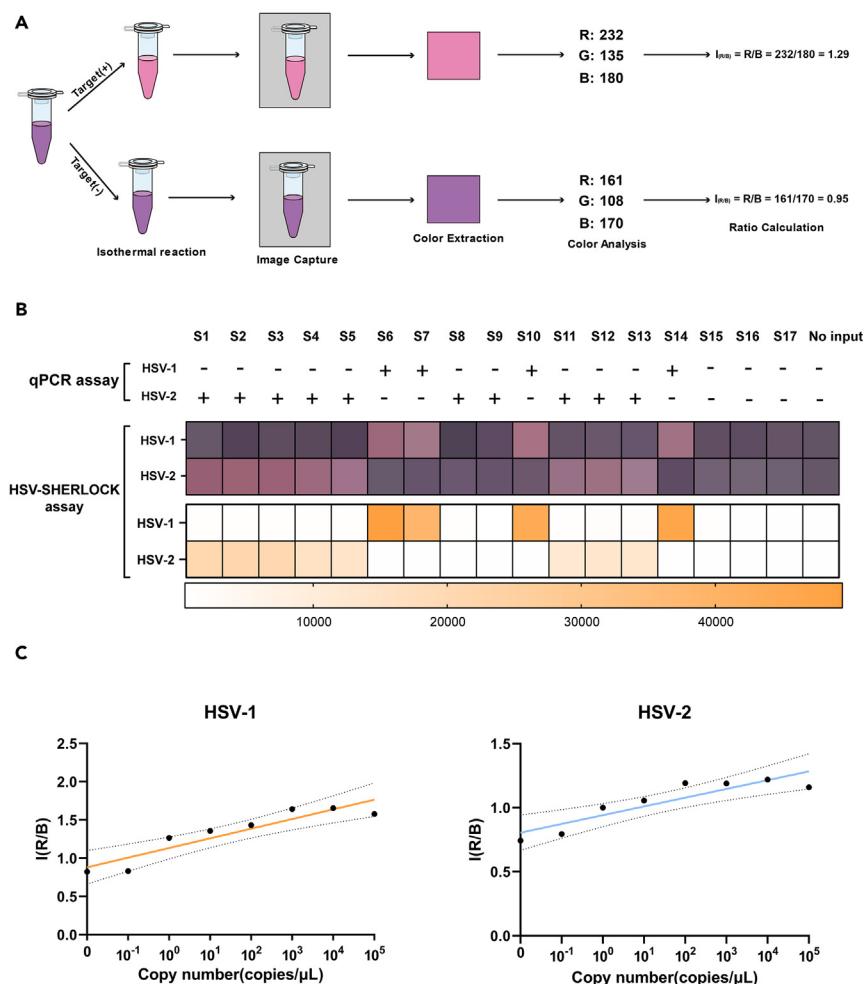


Figure 4. Results of colorimetric analysis

(A) The principle of colorimetric analysis with the Palette Cam app. When the RNA reporter was cleaved, the solution color changed from purple to pink. A smartphone camera was used to capture the reaction solution after incubation, and the app was used to analyze the image and extract the proportions of the three R(red), G(green) and B(blue) colors.

(B) The first row represents the detection and typing results obtained from the qPCR kit, which are displayed in the form of "+" and "-" to indicate positive and negative results, respectively. The second row represents the HSV-SHERLOCK assay colorimetric results, and the color block was extracted by the Palette Cam app; purple solution indicates a negative result, and pink indicates a positive result. The third row displays the fluorescence results by using the ROX channel on a CFX384 Touch Real-Time PCR Detection System (fluorescent signal was obtained at 1 h for the Cas13a reaction).

(C) Correlation of the copy number of *UL30* dsDNA with the ratio of R to B. Serially diluted aliquots of the *UL30* gene dsDNA template were detected with the HSV-SHERLOCK visualization reaction system. The free-app Palette Cam was used to extract the R/G/B values and calculate the ratio of R/B.

change in the reaction became more pronounced with an increase in ROX probe concentration, albeit with some background noise (Figure S3B). Based on the analysis of fluorescence intensity and background noise (Figures S3A and S3B), a concentration of 10 μ M for the ROX probe was chosen to establish the visualization system. To further optimize the input amount of RPA products as the detection targets in the visualization detection system, RPA products of 1.25, 2.5, and 5 μ L from the HSV-1 or HSV-2 template dsDNA with 10^5 and 10^1 copies/ μ L were added to the Cas13a system for the reaction. The results obtained from visual and fluorescent analysis of both HSV types (Figures S3C and S3D) demonstrated that the optimal input of RPA product was 5 μ L. When a 10 μ M ROX probe and an increased volume of 5 μ L input of RPA products were applied, the visualization system achieved a high sensitivity and could detect a single copy per μ L of HSV-1 or HSV-2 (Figures S4A and S4B).

We further validated the visual detection system using a small sample set that included 17 randomly selected samples from the previously mentioned 194 clinical samples. Among these samples, we identified 4 samples as positive for HSV-1, 8 samples as positive for HSV-2, and 5 samples as negative. The results obtained from the visual detection system were in complete agreement (100% concordance) with the commercial qPCR results (Figure 4B). Additionally, a photo of the visual results captured by a smartphone camera was provided (Figure S5). This confirms the reliability and consistency of the visual detection system in accurately detecting and genotyping HSV-1 and HSV-2 infections.

Adapting HSV-SHERLOCK for semiquantitative detection

To enable rapid and on-site quantification of HSV, we devised a method that utilizes smartphones and the Palette Cam application. By aligning the smartphone camera with the color change in HSV solutions, the Palette Cam application was used to capture the solution's color and analyze the red, green, blue (RGB) values. Specifically, the solution containing the RNA reporter labeled with the ROX fluorophore exhibited a purple color. Following the RPA, T7 transcription, and Cas13a detection steps of the positive HSV sample's *UL30* gene segment, the activated Cas13a protein cleaved the RNA reporter, causing the solution to transition from purple to pink. Utilizing a mobile phone camera, photographs are captured, and an application was employed to capture the color blocks within the solution. Subsequently, RGB ratio values were extracted, followed by the computation of the ratio between the R and B channels. As a result, HSV levels were assessed conveniently and measured in a semiquantitative manner (Figure 4A). As shown in Figure 4C, analysis of the red/blue (R/B) ratio of the solution against known copy numbers of standards revealed a strong correlation between the R/B ratio and the copy number of the target, with R^2 values of 0.8527 for HSV-1 and 0.8116 for HSV-2. These results highlight the potential of the HSV-SHERLOCK assay to detect HSV on-the-spot in a convenient and semiquantitative manner using a smartphone app.

DISCUSSION

HSV infection is the leading cause of genital herpes worldwide, with varying prevalence rates in different countries, including the United States, Mexico, African regions, and particularly in LMICs.^{6–8} A specialized device-free and easily accessible diagnostic method is necessary for detecting and monitoring HSV, especially in resource-limited settings.¹⁹ However, the existing diagnostic approaches used to detect HSV do not meet these criteria. In this study, we successfully developed a highly sensitive CRISPR-based dual-target diagnostic system for detecting and genotyping HSV-1 and HSV-2. We also adapted the assay for use with a mobile app or colorimetric readout, offering convenient and accurate detection capabilities.

Although NAAT-based analytical approaches exhibit high sensitivity and specificity for detecting and genotyping HSV, they are unsuitable for resource-constrained settings due to their complex workflow, requirement for a stringent operational environment, and intricate results, which are difficult to interpret.^{11,19} Our CRISPR-Cas-based assay simplifies the device requirements as the assay operates at an isothermal temperature and utilizes an alternative eye-visualization method. Thus, utilizing the assay in resource-limited regions is feasible. Compared to a commercial qPCR kit, the HSV-SHERLOCK assay demonstrated excellent performance in the detection of HSV-1, with a sensitivity of 96.15% (95% CI = 86.8–99.5) and a specificity of 100% (95% CI = 91–100). Similarly, for HSV-2, the assay showed a sensitivity of 95.15% (95% CI = 92.7–99.1) and a specificity of 100% (95% CI = 91–100). Furthermore, even though the testing input was 10-fold lower than that of commercial qPCR assays (1 μ L for our assay versus 10 μ L for the commercial qPCR assay, with 5 μ L allocated for HSV-1 detection and 5 μ L for HSV-2 detection), our assay still achieved remarkable PPV and NPV results compared to the commercial qPCR assay. Specifically, HSV-1 exhibits 100% PPV and 95.12% NPV, while HSV-2 demonstrates 100% PPV and 88.64% NPV. While previous isothermal diagnostics for HSV, such as LAMP, have been developed, their evaluation on clinical samples is lacking.²¹ In contrast to previous methods that required multiple primers in the reaction, our assay utilizes a single paired primer to amplify both types of HSV. Highly specific crRNA components are incorporated to distinguish the HSV types. Indeed, our assay effectively discriminates between positive and negative clinical samples within an 85-min runtime, with 60 min allocated for RPA and 25 min for Cas13a detection. This runtime is either shorter than or on par with the commercial qPCR assay (which takes approximately 90 min in this study). Given the redundancy of the RPA setup in this study, a 30-min RPA amplification period is deemed sufficient for target amplification,^{36–38} thus making the shortened runtime promising. Compared to current POCT methods such as helicase-dependent amplification, which has a runtime of 75 min,²³ and LAMP, which takes 45 min,²¹ our assay not only showcased a competitive turnaround time but also exhibited enhanced limit of detection, sensitivity, and specificity. Furthermore, the integration of our assay with straightforward sample processing significantly reduces the turnaround time compared to alternative methods that rely on commercial reagent kits or magnetic bead-based nucleic acid extraction. With its comparable performance to qPCR and the added advantage of an isothermal reaction, our assay provides accessible and accurate diagnosis in resource-limited settings.

The remarkable scalability of CRISPR-based technology has led to numerous advancements that enhance its potential for handheld use and POCT.^{31–33} By simply replacing the fluorescent moiety on the RNA reporter, we achieved visualized results without altering any reaction components, and the visual system exhibited excellent detection performance, displaying 100% concordance with clinical diagnostic results in a test involving 17 samples. To detect the visualized results in a semiquantitative manner using a simple method, we utilized a smartphone app employing RGB analysis. This approach demonstrated a favorable linear range ($R^2 = 0.8527$ for HSV-1, $R^2 = 0.8116$ for HSV-2); thus, the device shows great promise for performing semiquantitative assessments of HSV without complex instrumentation. Our study serves as a proof of concept for CRISPR-Cas-based HSV diagnostics, demonstrating its potential applicability in resource-limited settings. However, further work is needed to overcome challenges and translate this research into widely available POCTs.

In conclusion, our development of a CRISPR-Cas-based assay for simultaneous detection and genotyping of HSV holds great promise in enhancing HSV diagnosis, particularly in resource-constrained settings. This advancement shows the potential to significantly improve HSV diagnostics and contribute to more effective control strategies.

Limitations of the study

Although our approach displays promise, it is important to acknowledge certain limitations that require mitigation. Firstly, when compared to the prevailing POCT methods, we have not yet achieved a substantially reduced detection time. Given the inherent redundancy in reaction

time within the context of RPA, the prospect of attaining a more concise reaction time holds substantial potential. Secondly, our assay still necessitates the utilization of two distinct reaction vessels due to potential interference stemming from the intricate reaction components inherent to both RPA and CRISPR-based detection. It is our aspiration that, in the future, we can realize a streamlined one-pot reaction configuration.

STAR★METHODS

Detailed methods are provided in the online version of this paper and include the following:

- KEY RESOURCES TABLE
- RESOURCE AVAILABILITY
 - Lead contact
 - Materials availability
 - Data and code availability
- EXPERIMENTAL MODEL AND STUDY PARTICIPANT DETAILS
 - Human clinical specimens
 - Cell lines
- METHOD DETAILS
 - Clinical sample collection
 - Nucleic acid extraction from clinical samples
 - Double-stranded DNA template preparation and standard curve establishment
 - CRISPR–Cas13a-based fluorescent detection assay
 - Visualization of HSV-SHERLOCK detection
- QUANTIFICATION AND STATISTICAL ANALYSIS

SUPPLEMENTAL INFORMATION

Supplemental information can be found online at <https://doi.org/10.1016/j.isci.2023.108581>.

ACKNOWLEDGMENTS

This study was supported by Guangzhou Science and Technology Plan Project (No. 202201000007) and the National Natural Science Foundation of China Grant (No. 82302579). The funders of this study only provided funding, and had no role in the study design, data analysis, data interpretation, or editing and reviewing of the manuscript. We express our special gratitude to the Clinical Laboratory of the Dermatology Hospital of Southern Medical University for providing us with the clinical samples.

AUTHOR CONTRIBUTIONS

H.Zheng, W.C., X.Y., and H.L. conceptualized the study. W.C., X.Y., and H.L. designed the experiments. X.Y., H.L., H.Zhou, Z.Z., and Z.F. performed most of the experiments, data analysis, and data interpretation. H.Zhou, Z.Z., and Y.L. performed sample collection and DNA extraction. X.Y. and H.L. drafted the manuscript. All authors contributed to editing, reviewing of the manuscript, and approved the final version of the manuscript.

DECLARATION OF INTERESTS

The authors declare no interest in conflicts.

Received: July 26, 2023

Revised: October 2, 2023

Accepted: November 23, 2023

Published: November 27, 2023

REFERENCES

1. Whitley, R.J., Kimberlin, D.W., and Roizman, B. (1998). Herpes simplex viruses. *Clin. Infect. Dis.* 26, 541–553. quiz 554–555.
2. Whitley, R.J., and Roizman, B. (2001). Herpes simplex virus infections. *Lancet* 357, 1513–1518.
3. Efsthathiou, S., Field, H.J., Griffiths, P.D., Kern, E.R., Sacks, S.L., Sawtell, N.M., and Stanberry, L.R. (1999). Herpes simplex virus latency and nucleoside analogues. *Antiviral Res.* 41, 85–100.
4. Gupta, R., Warren, T., and Wald, A. (2007). Genital herpes. *Lancet* 370, 2127–2137.
5. Johnston, C., Magaret, A., Son, H., Stern, M., Rathbun, M., Renner, D., Szpara, M., Gunby, S., Ott, M., Jing, L., et al. (2022). Viral Shedding 1 Year Following First-Episode Genital HSV-1 Infection. *JAMA* 328, 1730–1739.
6. James, C., Harfouche, M., Welton, N.J., Turner, K.M., Abu-Raddad, L.J., Gottlieb, S.L., and Looker, K.J. (2020). Herpes simplex virus: global infection prevalence and incidence estimates, 2016. *Bull. World Health Organ.* 98, 315–329.

7. Tuddenham, S., Hamill, M.M., and Ghanem, K.G. (2022). Diagnosis and Treatment of Sexually Transmitted Infections: A Review. *JAMA* 327, 161–172.
8. Silva, S., Ayoub, H.H., Johnston, C., Atun, R., and Abu-Raddad, L.J. (2022). Estimated economic burden of genital herpes and HIV attributable to herpes simplex virus type 2 infections in 90 low- and middle-income countries: A modeling study. *PLoS Med.* 19, e1003938.
9. Patel, R., Green, J., Clarke, E., Seneviratne, K., Abbt, N., Evans, C., Bickford, J., Nicholson, M., O'Farrell, N., Barton, S., et al. (2015). 2014 UK national guideline for the management of anogenital herpes. *Int. J. STD AIDS* 26, 763–776.
10. LeGoff, J., Péré, H., and Bélec, L. (2014). Diagnosis of genital herpes simplex virus infection in the clinical laboratory. *Virol. J.* 11, 83.
11. Anderson, N.W., Buchan, B.W., and Ledebor, N.A. (2014). Light microscopy, culture, molecular, and serologic methods for detection of herpes simplex virus. *J. Clin. Microbiol.* 52, 2–8.
12. Nath, P., Kabir, M.A., Doust, S.K., and Ray, A. (2021). Diagnosis of Herpes Simplex Virus: Laboratory and Point-of-Care Techniques. *Infect. Dis. Rep.* 13, 518–539.
13. Granato, P.A., Alkins, B.R., Yen-Lieberman, B., Greene, W.H., Connolly, J., Buchan, B.W., and Ledebor, N.A. (2015). Comparative Evaluation of AmpliVue HSV 1+2 Assay with ELVIS Culture for Detecting Herpes Simplex Virus 1 (HSV-1) and HSV-2 in Clinical Specimens. *J. Clin. Microbiol.* 53, 3922–3925.
14. Cao, G., Tan, C., Zhang, Y., Kong, X., Sun, X., Ma, Y., Chen, J., and Guan, M. (2019). Digital droplet polymerase chain reaction analysis of common viruses in the aqueous humour of patients with Posner-Schlossman syndrome in Chinese population. *Clin. Exp. Ophthalmol.* 47, 513–520.
15. Gitman, M.R., Ferguson, D., and Landry, M.L. (2013). Comparison of Simplex HSV 1 & 2 PCR with culture, immunofluorescence, and laboratory-developed TaqMan PCR for detection of herpes simplex virus in swab specimens. *J. Clin. Microbiol.* 51, 3765–3769.
16. Slinger, R., Amrud, K., Sant, N., Ramotar, K., and Desjardins, M. (2019). A comparison of the Quidel Solana HSV 1 + 2/VZV Assay, the Focus Diagnostics Simplex HSV 1 & 2 Direct Assay and the Luminex Aries HSV 1&2 Assay for detection of herpes simplex virus 1 and 2 from swab specimens. *J. Clin. Virol.* 113, 35–38.
17. Levin, M.J., Weinberg, A., and Schmid, D.S. (2016). Herpes Simplex Virus and Varicella-Zoster Virus. *Microbiol. Spectr.* 4, DMIH2-0017-2015.
18. Fatahzadeh, M., and Schwartz, R.A. (2007). Human herpes simplex virus infections: epidemiology, pathogenesis, symptomatology, diagnosis, and management. *J. Am. Acad. Dermatol.* 57, 737–763. quiz 764–766.
19. Kang, T., Lu, J., Yu, T., Long, Y., and Liu, G. (2022). Advances in nucleic acid amplification techniques (NAATs): COVID-19 point-of-care diagnostics as an example. *Biosens. Bioelectron.* 206, 114109.
20. Cassidy, A., Parle-McDermott, A., and O'Kennedy, R. (2021). Virus Detection: A Review of the Current and Emerging Molecular and Immunological Methods. *Front. Mol. Biosci.* 8, 637559.
21. Nahar, S., Ahmed, M.U., Safavieh, M., Rochette, A., Toro, C., and Zourob, M. (2015). A flexible and low-cost polypropylene pouch for naked-eye detection of herpes simplex viruses. *Analyst* 140, 931–937.
22. Ooi, K.H., Liu, M.M., Moo, J.R., Nimsamer, P., Payungporn, S., Kaewsapaks, P., and Tan, M.H. (2022). A Sensitive and Specific Fluorescent RT-LAMP Assay for SARS-CoV-2 Detection in Clinical Samples. *ACS Synth. Biol.* 11, 448–463.
23. Lemieux, B., Li, Y., Kong, H., and Tang, Y.W. (2012). Near instrument-free, simple molecular device for rapid detection of herpes simplex viruses. *Expert Rev. Mol. Diagn.* 12, 437–443.
24. Huang, T., Zhang, R., and Li, J. (2023). CRISPR-Cas-based techniques for pathogen detection: Retrospect, recent advances, and future perspectives. *J. Adv. Res.* 50, 69–82.
25. Li, L., Shen, G., Wu, M., Jiang, J., Xia, Q., and Lin, P. (2022). CRISPR-Cas-mediated diagnostics. *Trends Biotechnol.* 40, 1326–1345.
26. Chen, W., Luo, H., Zeng, L., Pan, Y., Parr, J.B., Jiang, Y., Cunningham, C.H., Hawley, K.L., Radolf, J.D., Ke, W., et al. (2022). A suite of PCR-LwCas13a assays for detection and genotyping of *Treponema pallidum* in clinical samples. *Nat. Commun.* 13, 4671.
27. Gootenberg, J.S., Abudayyeh, O.O., Lee, J.W., Essletzbichler, P., Dy, A.J., Joung, J., Verdine, V., Donghia, N., Daringer, N.M., Freije, C.A., et al. (2017). Nucleic acid detection with CRISPR-Cas13a/C2c2. *Science* 356, 438–442.
28. Ackerman, C.M., Myhrvold, C., Thakku, S.G., Freije, C.A., Metsky, H.C., Yang, D.K., Ye, S.H., Boehm, C.K., Kosoko-Thoroddsen, T.S.F., Kehe, J., et al. (2020). Massively multiplexed nucleic acid detection with Cas13. *Nature* 582, 277–282.
29. Luo, H., Chen, W., Mai, Z., Yang, J., Lin, X., Zeng, L., Pan, Y., Xie, Q., Xu, Q., Li, X., et al. (2022). Development and application of Cas13a-based diagnostic assay for *Neisseria gonorrhoeae* detection and azithromycin resistance identification. *J. Antimicrob. Chemother.* 77, 656–664.
30. Patchsung, M., Jantarug, K., Pattama, A., Aphicho, K., Suraritdechachai, S., Meesawat, P., Sappakhaw, K., Leelahakorn, N., Ruenkam, T., Wongsatit, T., et al. (2020). Clinical validation of a Cas13-based assay for the detection of SARS-CoV-2 RNA. *Nat. Biomed. Eng.* 4, 1140–1149.
31. Fozouni, P., Son, S., Díaz de León Derby, M., Knott, G.J., Gray, C.N., D'Ambrosio, M.V., Zhao, C., Switz, N.A., Kumar, G.R., Stephens, S.I., et al. (2021). Amplification-free detection of SARS-CoV-2 with CRISPR-Cas13a and mobile phone microscopy. *Cell* 184, 323–333.e329.
32. Welch, N.L., Zhu, M., Hua, C., Weller, J., Mirhashemi, M.E., Nguyen, T.G., Mantena, S., Bauer, M.R., Shaw, B.M., Ackerman, C.M., et al. (2022). Multiplexed CRISPR-based microfluidic platform for clinical testing of respiratory viruses and identification of SARS-CoV-2 variants. *Nat. Med.* 28, 1083–1094.
33. Najjar, D., Rainbow, J., Sharma Timilsina, S., Jolly, P., de Puig, H., Yafia, M., Durr, N., Sallum, H., Alter, G., Li, J.Z., et al. (2022). A lab-on-a-chip for the concurrent electrochemical detection of SARS-CoV-2 RNA and anti-SARS-CoV-2 antibodies in saliva and plasma. *Nat. Biomed. Eng.* 6, 968–978.
34. Wu, X., Chan, C., Springs, S.L., Lee, Y.H., Lu, T.K., and Yu, H. (2022). A warm-start digital CRISPR/Cas-based method for the quantitative detection of nucleic acids. *Anal. Chim. Acta* 1196, 339494.
35. Dou, B., Zhang, Y., Gao, H., Zhang, S., Zheng, J., Lu, X., Liu, S., Zhou, H., and Hun, X. (2023). CRISPR/Cas12a-based MUSCA-PEC strategy for HSV-1 assay. *Anal. Chim. Acta* 1250, 340955.
36. Lobato, I.M., and O'Sullivan, C.K. (2018). Recombinase polymerase amplification: Basics, applications and recent advances. *Trends Anal. Chem.* 98, 19–35.
37. Cao, Y., Zheng, K., Jiang, J., Wu, J., Shi, F., Song, X., and Jiang, Y. (2018). A novel method to detect meat adulteration by recombinase polymerase amplification and SYBR green I. *Food Chem.* 266, 73–78.
38. Tan, M., Liao, C., Liang, L., Yi, X., Zhou, Z., and Wei, G. (2022). Recent advances in recombinase polymerase amplification: Principle, advantages, disadvantages and applications. *Front. Cell. Infect. Microbiol.* 12, 1019071.
39. Buderer, N.M. (1996). Statistical methodology: I. Incorporating the prevalence of disease into the sample size calculation for sensitivity and specificity. *Acad. Emerg. Med.* 3, 895–900.
40. Legoff, J., Bouhlal, H., Grésenguet, G., Weiss, H., Khonde, N., Hocini, H., Désiré, N., Si-Mohamed, A., de Dieu Longo, J., Chemin, C., et al. (2006). Real-time PCR quantification of genital shedding of herpes simplex virus (HSV) and human immunodeficiency virus (HIV) in women coinfecting with HSV and HIV. *J. Clin. Microbiol.* 44, 423–432.
41. Lieveld, M., Carregosa, A., Benoy, I., Redzic, N., Berth, M., and Vanden Broeck, D. (2017). A high resolution melting (HRM) technology-based assay for cost-efficient clinical detection and genotyping of herpes simplex virus (HSV)-1 and HSV-2. *J. Virol. Methods* 248, 181–186.
42. Xie, S., Tao, D., Fu, Y., Xu, B., Tang, Y., Steinaa, L., Hemmink, J.D., Pan, W., Huang, X., Nie, X., et al. (2022). Rapid Visual CRISPR Assay: A Naked-Eye Colorimetric Detection Method for Nucleic Acids Based on CRISPR/Cas12a and a Convolutional Neural Network. *ACS Synth. Biol.* 11, 383–396.
43. DeLong, E.R., DeLong, D.M., and Clarke-Pearson, D.L. (1988). Comparing the areas under two or more correlated receiver operating characteristic curves: a nonparametric approach. *Biometrics* 44, 837–845.

STAR★METHODS

KEY RESOURCES TABLE

REAGENT or RESOURCE	SOURCE	IDENTIFIER
Critical commercial assays		
Nucleic Acid Extraction Buffer	Triplex International Biosciences, China	N/A
Q5 high-fidelity DNA polymerase	New England Biolabs, MA, USA	Cat# M0492S
Universal DNA Gel Extraction Kit	TIANGEN, Beijing, China	Cat# DP214-03
DNeasy Blood & Tissue Kit	QIAGEN, Hilden, Germany	Cat# 69506
dd PCR Supermix for Probes (No dUTP)	Bio-Rad, CA, USA	Cat# 186-3023
TwistAmp Basic Kit	TwistDx, Maidenhead, Berkshire, UK	Cat# TABAS03KIT
Tris-HCl (pH 7.5)	Invitrogen, CA, USA	Cat# 15567-027
Ribonucleotide Solution Mix	New England Biolabs, MA, USA	Cat# N0466L
Murine RNase inhibitor	New England Biolabs, MA, USA	Cat# M0314L
T7 RNA Polymerase	New England Biolabs, MA, USA	Cat# M0251L
LwCas13a	GenScript, China	Cat# Z03486
HiScribe T7 Quick High Yield RNA Synthesis Kit	New England Biolabs, MA, USA	Cat# E2050S
RNA XP Clean Beads	Beckman, CA, USA	Cat# A63987
Qubit RNA HS Assay Kit	Thermo Fisher Scientific, Waltham, MA, USA	Cat# Q32852
Experimental models: Cell lines		
HeLa cell line	CCDCC, Wuhan, China	Cat# GDC0009; RRID: CVCL_0030
Oligonucleotides		
RPA-F1: GAAATTAATACGACTCACTATAGGGTG TTTGAAATAACGCCAAGATCACCGAGAGTC	This paper	N/A
RPA-F2: GAAATTAATACGACTCACTATAGGGAA GGCCCTGTTTGAAATAACGCCAAGATCAC	This paper	N/A
RPA-F3: GAAATTAATACGACTCACTATAGGGA ATAACGCCAAGATCACCGAGAGTCTGTAA	This paper	N/A
RPA-F4: GAAATTAATACGACTCACTATAGGGG CCCTGTTTGAAATAACGCCAAGATCACCGAG	This paper	N/A
RPA-F5: GAAATTAATACGACTCACTATAGGGTG GAAATAACGCCAAGATCACCGAGAGTCTGT	This paper	N/A
RPA-F6: GAAATTAATACGACTCACTATAGGGC GCCAAGATCACCGAGAGTCTGTAAAGAG	This paper	N/A
RPA-R1: CTCTATGCAACATTGACGAGTTTC CTCCGCCGTA	This paper	N/A
RPA-R2: CTATGCAACATTGACGAGTTTCC TCCGCCGTA	This paper	N/A
RPA-R3: ATGCAACATTGACGAGTTTCCTCCGCCGTAGC	This paper	N/A
RPA-R4: CAAAGGCTCTATGCAACATTGACGAGTTTCCT	This paper	N/A
RPA-R5: CAAAGGCTCTATGCAACATTGACGAGTTTCCTCC	This paper	N/A
RPA-R6: AAGGCTCTATGCAACATTGACGA GTTTCCTC	This paper	N/A
PCR-F: GAAATTAATACGACTCACTATAGGGGTTTC CGCTCAACACGACTATT	This paper	N/A

(Continued on next page)

Continued

REAGENT or RESOURCE	SOURCE	IDENTIFIER
PCR-R: CATTGACGAGTTTCCTCCGC	This paper	N/A
ddPCR-F: GCCAAGATCACCGAGAGTCTGT	This paper	N/A
ddPCR-R: CATTGACGAGTTTCCTCCGC	This paper	N/A
ddPCR-probe: 6FAM-ACGACGTGGCCGCGCG GCTC-BHQ1	This paper	N/A
HSV1-crRNA1: ACUUCGGGAUAAACCUUUUUAACAGAC	This paper	N/A
HSV1-crRNA2: CCACACUUCGGGAUAAACCUUUUUAAC	This paper	N/A
HSV1-crRNA3: GCCACACUUCGGGAUAAACCUUUUUA	This paper	N/A
HSV1-crRNA4: UGCCACACUUCGGGAUAAACCUUUUUA	This paper	N/A
HSV1-crRNA5: GUGCCACACUUCGGGAUAAACCUUUUU	This paper	N/A
HSV1-crRNA6: GGUGCCACACUUCGGGAUAAACCUUUU	This paper	N/A
HSV1-crRNA7: GGGUGCCACACUUCGGGAUAAACCUUU	This paper	N/A
HSV1-crRNA8: GGGUGCCACACUUCGGGAUAAACCUU	This paper	N/A
HSV2-crRNA1: GUCUCGGGAUAAACCUCUUUAACAGAC	This paper	N/A
HSV2-crRNA2: CCACGUCUCGGGAUAAACCUCUUUAAC	This paper	N/A
HSV2-crRNA3: GCCACGUCUCGGGAUAAACCUCUUUA	This paper	N/A
HSV2-crRNA4: UGCCACGUCUCGGGAUAAACCUCUUUA	This paper	N/A
HSV2-crRNA5: GUGCCACGUCUCGGGAUAAACCUCUUU	This paper	N/A
HSV2-crRNA6: GGUGCCACGUCUCGGGAUAAACCUCUU	This paper	N/A
HSV2-crRNA7: GGGUGCCACGUCUCGGGAUAAACCUCU	This paper	N/A
HSV2-crRNA8: GGGUGCCACGUCUCGGGAUAAACCUC	This paper	N/A
HSV1-crRNA(22 nt): CCACACUUCGGGAU UAAACCUU	This paper	N/A
HSV1-crRNA(24 nt): UGCCACACUUCGGGAUAAACCUU	This paper	N/A
HSV1-crRNA(26 nt): GGUGCCACACUUCGGGAUAAACCUU	This paper	N/A
HSV1-crRNA(28 nt): GGGUGCCACACUUCGGGAUAAACCUU	This paper	N/A
HSV1-crRNA(30 nt): GGGGUGCCACACUUCGGGAUAAACCUU	This paper	N/A
HSV2-crRNA(22 nt): CCACGUCUCGGGAUAAACCUC	This paper	N/A

(Continued on next page)

Continued

REAGENT or RESOURCE	SOURCE	IDENTIFIER
HSV2-crRNA(24 nt): UGCCACGUCUCGGAAUAAACCUC	This paper	N/A
HSV2-crRNA(26 nt): GGUGCCACGUCUCGGAAUAAACCUC	This paper	N/A
HSV2-crRNA(28 nt): GGGGUGCCACGUCUCGGAAUAAACCUC	This paper	N/A
HSV2-crRNA(30 nt): GGGGGGUGCCACGUCUCGGAAUAAACCUC	This paper	N/A

Software and algorithms

Droplet Digital PCR System	Bio-Rad, Hercules, CA, USA	Cat# QX200; RRID: SCR_019707
SnapGene	https://www.snapgene.com/	N/A
Prism 9	https://www.graphpad.com/	N/A
MedCalc	https://www.medcalc.org/	N/A
Palette Cam	https://apps.apple.com/us/app/palette-cam/id1102067114	N/A

Deposited data

UL30 gene segment of HSV-1/2	this study	Genbank: accession code OR345521, OR345522
Dataset for this paper	this study	Mendeley Data: https://doi.org/10.17632/zk9kf6dkfg.1

RESOURCE AVAILABILITY**Lead contact**

Further information and requests for resources and reagents should be directed to and will be fulfilled by the lead contact, Heping Zheng (zhengheping@smu.edu.cn).

Materials availability

This study did not generate new unique reagents.

Data and code availability

- Data - DNA sequencing data generated in this study have been deposited in the GenBank database and are publicly available as of the date of publication. Accession numbers are listed in the [key resources table](#). The dataset for this paper has been deposited at Mendeley and are publicly available as of the date of publication. The DOI is listed in the [key resources table](#).
- Code - No code was generated during the course of this study.
- Other - Any additional information required to reanalyze the data reported in this paper is available from the [lead contact](#) upon request.

EXPERIMENTAL MODEL AND STUDY PARTICIPANT DETAILS**Human clinical specimens**

All clinical specimens were obtained from patients at the Southern Medical University Dermatology Hospital and underwent ethical scrutiny, receiving approval from the Ethics Review Committee of the Southern Medical University Dermatology Hospital (GDDHLS-2020056, 2021071). This study exclusively utilized residual samples diagnosed in the clinical laboratory to validate the detection capability of our assay, with no alterations to clinical care. The participants included 107 males, 84 females, and 3 with unavailable information, and all of Chinese origin. Demographic details are accessible in [Table S1](#).

Cell lines

The HeLa cell line (CCDCC, Wuhan, China) employed in this study underwent DNA extraction following the manufacturer's stipulations, utilizing the DNeasy Blood & Tissue Kit (QIAGEN). The extracted cellular DNA was subsequently incorporated into the HSV standard, simulating the human genetic background.

METHOD DETAILS

Clinical sample collection

In this study, we constructed and evaluated the performance of HSV detection and genotyping assays using clinical samples from the Dermatology Hospital of Southern Medical University in Guangdong Province, China. Based on the 2016 WHO global prevalence rates for HSV infection (HSV-1 at 67% and HSV-2 at 13.2%) and conducting a small sample size test, we assumed 95% expected sensitivity and specificity with a 95% confidence interval. Following the method described by Buderer,³⁹ we calculated that a sample size of 56 is required for testing HSV-1, and 139 for testing HSV-2. A total of 194 clinical swab specimens were collected for this subject, including 52 HSV-1-positive samples, 103 HSV-2-positive samples, and 39 HSV1/2-negative samples, and all samples were confirmed by a commercial qPCR kit (Triplex International Biosciences) with Roche Cobas z480 (relevant information including sex, age, race, sampling sites, and more, can be found in Table S1). The criteria of this subject for clinical enrollment include confirmation that the sample was positive by qPCR or the clinical manifestations were suspected to be HSV infections. The clinical samples were chosen randomly from a large pool, and the experimenters conducting the experiments were not blinded. A testing set with ten prevalent urogenital pathogens including *Herpes Simplex Virus I*, *Herpes Simplex Virus II*, *Treponema pallidum*, *Chlamydia trachomatis*, *Neisseria gonorrhoeae*, *Escherichia coli*, *Candida albicans*, *Enterococcus faecalis*, *Ureaplasma urealyticum*, and *Trichomonas vaginalis*, was collected to validate the specificity of the SHERLOCK assay.

Nucleic acid extraction from clinical samples

The nucleic acids of clinical specimens were extracted using a boiling pyrolysis method. In brief, 1 mL of sterilized saline was added to the swab after the sample were collected in a 1.5 mL centrifuge tube, the sample were centrifuged, and the supernatant was removed. Then, 50 μ L of nucleic acid extract (from Herpes simplex Virus Nucleic Acid Test Kit (Fluorescent PCR) (Triplex International Biosciences)) was added to the precipitate, vortexed thoroughly and treated at 100°C for 10 min. The processed product was saved for subsequent experiments.

Double-stranded DNA template preparation and standard curve establishment

The target for the two types of HSV *UL30* gene conserved regions^{40,41} was amplified by Q5 high-fidelity DNA polymerase (New England Biolabs) in a 50 μ L volume, comprising of 10 μ L of 5X Q5 Reaction buffer, 1 μ L of 10 μ M dNTPs, 2.5 μ L of 10 μ M universal primers, 2 μ L of input DNA, 0.5 μ L of Q5 High-Fidelity DNA Polymerase and 31.5 μ L of ddH₂O to further evaluate the LOD of this assay. Subsequently, 1% agarose gel was used to determine the correct fragments (Figure S2A) and the target dsDNA template was reclaimed using the Universal DNA Gel Extraction Kit (TIANGEN) according to the manufacturer's protocol. The sequences of the target were validated by Sanger sequencing (Sangon Biotech) (Figure S2B). DNA sequencing data generated in this study have been deposited in the GenBank database under accession code OR345521 and OR345522. Then a 10-fold gradient dilution from 1 $\times 10^5$ copies/ μ L to 1 $\times 10^{-1}$ copies/ μ L was used, and human genome DNA (extracted from the HeLa cell line, RRID: CVCL_0030) was added to 1 ng/ μ L to simulate the human genome DNA background in clinical samples. To determine the actual copy number of samples, ddPCR was used in a 20 μ L total reaction as follows: 10 μ L ddPCR Supermix for Probes (No dUTP) (Bio-Rad), 0.9 μ L of 10 μ M universal primers, 0.5 μ L of 10 μ M universal probes, 1 μ L of DNA template, and 6.7 μ L of ddH₂O, following the subsequent steps on Droplet Digital PCR System (RRID: SCR_019707) to generate droplets, seal, PCR procedure, and analysis (Figure S2C).

CRISPR-Cas13a-based fluorescent detection assay

All the oligonucleotides were synthesized by Sangon Biotech Co. Ltd. (Shanghai, China), and the sequences are shown in Table S2. The crRNAs and RPA primers were designed using SnapGene (v4.1.9) and NCBI BLAST. A pair of universal primers based on the high genomic similarity of the HSV genome was devised.⁴ The synthesized single-stranded oligonucleotide (100 μ M) which contains the complementary sequences of the T7 promoter, spacer, and core sequences was annealed with a short T7 promoter (100 μ M) using a gradient annealing process (95°C–25°C) with a cooling rate of 1 °C/min. Subsequently, the products were transcribed into crRNA for 16 h at 37°C by using the HiScribe T7 Quick High Yield RNA Synthesis Kit (New England Biolabs). Then, the crRNAs were purified by RNA XP Clean Beads (Beckman) and quantified with the Qubit RNA HS Assay Kit (Thermo Fisher Scientific). Finally, the crRNAs were stored at –20°C until use. The TwistAmp Basic Kit (TwistDx) was used for amplification and included the following components: 29.5 μ L TwistAmp rehydration buffer, 2.5 μ L of each 10 μ M universal primer, 11 μ L ddH₂O, and 2.5 μ L TwistAmp magnesium acetate (280 mM). Then, the master mix was transferred into one TwistAmp pellet and divided into 24- μ L aliquots, followed by the addition of 1 μ L clinical sample DNA to form a 25 μ L reaction mix. Incubating at 37°C for 1 h and then transferring 1.25 μ L of RPA products to LwCas13a collateral detection. The LwCas13a reaction comprises the following components: 40 mM Tris-HCl (pH 7.5) (Invitrogen), 9 mM MgCl₂, 1 mM Ribonucleotide Solution Mix (New England Biolabs), 2000 U/mL Murine RNase inhibitor (New England Biolabs), 1500 U/mL T7 RNA Polymerase (New England Biolabs), 225 nM HSV-1 or HSV-2 crRNA, 45 nM LwCas13a (GenScript; Z03486-500) and 125 nM collateral RNA reporter (5'-6FAM-UUUUU-BHQ1-3'). The reaction mixture was incubated for 1 h at 37°C on a 96 well half-area microplate (Corning) for fluorescent kinetics analysis with measurements at excitation/emission wavelengths of 490 nm/520 nm every 5 min.

Visualization of HSV-SHERLOCK detection

To establish a visual detection assay, we selected ROX as the fluorophore modification of the RNA reporter (5'-ROX-UUUUU-BHQ2-3') according to Xie's reporter⁴² instead of the fluorescence reporter at 10 μ M and added 5 μ L of the RPA products under the same conditions

as mentioned above for visualization. When the target was present, the color of the reaction mixture underwent a noticeable visual transformation from purple to pink. The Palette Cam application (downloaded from the smartphone's app store, <https://apps.apple.com/us/app/palette-cam/id1102067114>) was manipulated to simplify the analysis in the Red, Green, Blue (RGB) color mode. The fluorescence signal was acquired every 5 min for 1 h using the ROX channel on a CFX384 Touch Real-Time PCR Detection System (Bio-Rad) and photographs were captured using an iPhone.

QUANTIFICATION AND STATISTICAL ANALYSIS

The XY-axis fitting curve, statistical analysis, and visualization were performed with Prism 9 software (v9.0.0). Data are presented as the measured mean \pm SEM. The quantified mean differences were determined using a one-way ANOVA, with significance considered at a p value <0.05 . The receiver operating characteristic (ROC) curve was constructed with a confidence interval of 95% (DeLong et al. method⁴³) by MedCalc software (v20.0). The positive predictive value (PPV), negative predictive value (NPV), accuracy, and Kappa coefficient (κ -value) were calculated and processed using MedCalc software (v20.0).